The torsional barriers of two equivalent methyl internal rotations in 2,5-dimethylfuran investigated by microwave spectroscopy

Vinh Van, Jonas Bruckhuisen, Wolfgang Stahl, Vadim Ilyushin, Ha Vinh Lam Nguyen

The torsional barriers of two equivalent methyl internal rotations in 2,5-dimethylfuran as observed by microwave spectroscopy

Vinh Van,[1] Jonas Bruckhuisen,[1] Wolfgang Stahl,[1] Vadim Ilyushin,[2] and Ha Vinh Lam Nguyen[3,*]

[1] Institute of Physical Chemistry, RWTH Aachen University, Landoltweg 2, 52074 Aachen, Germany

[2] Institute for Radio Astronomy of NASU, Mystetstv str. 4, 61002 Kharkiv, Ukraine

[3] Laboratoire Interuniversitaire des Systèmes Atmosphériques (LISA), CNRS UMR 7583, Université Paris-Est Créteil, Université Paris Diderot, 61 avenue du Général de Gaulle, 94010 Créteil cedex, France

* Corresponding author: Dr. Ha Vinh Lam Nguyen

Email: lam.nguyen@lisa.u-pec.fr

Abstract

The microwave spectrum of 2,5-dimethylfuran was recorded using two pulsed molecular jet Fourier transform microwave spectrometers which cover the frequency range from 2 - 40 GHz. The internal rotations of two equivalent methyl tops with a barrier height of approximately 439.15 cm^{-1} introduce torsional splittings of all rotational transitions in the spectrum. For the spectral analysis, two different computer programs were applied and compared, the *PAM-C_{2v}-2tops* code based on the principal axis method which treats several torsional states simultaneously, and the *XIAM* code based on the combined axis method, yielding accurate rotational and centrifugal distortion constants. The experimental work was supplemented by quantum chemical calculations. Two-dimensional potential energy surfaces depending on the torsional angles of both methyl groups were calculated and parametrized.

Keywords: microwave spectroscopy, rotational spectroscopy, internal rotation

1. Introduction

The petroleum produced from raw resources is currently threatened by the fossil limits, decreasing accessibility and hazardous effects on environment. The fulfilment of ever growing needs for petroleum today strongly demands renewable sources. Several studies have shown that the conversion of biomass such as hexose (e.g. fructose or glucose) into liquid fuels is a promising way to produce renewable liquid fuel, with 2,5-dimethylfuran (DMF) as the most attractive product [1,2]. Compared to ethanol known as the unique renewable fuel produced in large quantities so far, DMF promises a distinction by its nearly ideal boiling point (92–94°C at 1013 mbar) and its high research octane number (RON = 119) [3]. Besides, the energy content of 31.5 MJ/L is similar to that of gasoline (35 MJ/L) and 40% greater than that of ethanol (23 MJ/L) [4]. In addition, it is immiscible with water and easier to blend with gasoline than ethanol.

Despite its widespread use, almost nothing is known about the gas phase molecular structure and internal dynamics of DMF. We considered it worthwhile to study the title molecule by pulsed molecular jet Fourier transform microwave (FTMW) spectroscopy with quantum chemical calculations as a helpful support to obtain this important information. From the structural point of view, DMF is a derivative of furan with two methyl substitutions on the second and the fifth ring positions. The methyl groups are thus equivalent. Concerning the internal dynamics, when starting this work, we expected that splittings arising from the internal rotations of the two equivalent methyl groups are resolvable. Two programs treating such large amplitude motion problems, the *XIAM* [5] and *PAM-*C_{2v}*-2tops* codes [6] are

applied to reproduce the experimental spectrum. The results obtained from these two codes are compared with each other and with those from quantum chemical calculations.

2. Quantum chemical calculations

2.1. Geometry optimizations

Similar to the case of furan, the heavy atoms of DMF share a symmetry plane because of the π electron delocalization of two conjugated double bonds. This constraint confines the structural analysis to only one starting geometry, which was fully optimized at the MP2/6-311++G(d,p) level of theory using the *Gaussian09* package [7]. In almost all recent investigations we used this method-basis set combination because of its optimal compromise between accuracy and speed of the calculations [8-10]. The optimized structure in the principal axes of inertia is presented in Fig. 1; the nuclear Cartesian coordinates are available in Table S-1 in the Supplementary Material. Calculations at various combinations of methods (HF, B3LYP, M06-2X, MP2, and CCSD) and Pople and Dunning basis sets [11,12] were performed in addition to check for convergence. The rotational constants obtained at different levels of theory are summarized in Table S-2. All calculated values in the following sections will refer to the MP2/6-311++G(d,p) level, if not stated otherwise.

2.2. Methyl internal rotations

DMF possesses a C_{2v} symmetry and two equivalent methyl rotors. The rotational transitions of such molecule exhibit fine splittings into four torsional components, which can be labeled as (00), (01), (11), and (12) by writing G_{36} as the semi-direct product $(\boldsymbol{C_3^I} \times \boldsymbol{C_3^I}) \ltimes \boldsymbol{C_{2v}}$, as introduced in Ref. [13], where $\boldsymbol{C_3^I}$ is the intrinsic (superscript I) $\boldsymbol{C_3}$ group of an internal rotor, which is an invariant subgroup of G_{36}. We will use the notation (00), (01), (11), and (12) throughout the present work.

The torsional splittings mainly depend on the orientations of the methyl groups in the molecule and the barriers hindering the internal rotations. While the former can be often

calculated well by geometry optimizations, predicting the barrier heights is a much more difficult task. The predicted values vary in a wide range and depend strongly on the level of theory in use [13,14]. A level that yields a reasonable value for one methyl group may fail for another methyl group, even in the same molecule [15]. High level quantum chemical methods such as diffusion quantum Monte Carlo and coupled cluster are more time-consuming, on the other hand are not in better agreement with the experiment than calculations at some levels using the MP2 method [16]. On the other hand, results from quantum chemical calculations often give the correct order of magnitude (low, intermediate, or high) of the barrier heights, which is sufficient to get a start on the spectral assignment.

For DMF, we calculated the barrier heights of the equivalent methyl groups by geometry optimizations to a first order transition state of one methyl group using the Berny algorithm [17] at various levels of theory already mentioned in Section 2.1. The angles between the internal rotor axes and the *a*-principal axis as well as the calculated V_3 potentials are also given in Table S-2 in the Supplementary Material.

2.3. Potential energy surfaces

Two-dimensional potential energy surfaces (2D-PES) depending on the dihedral angles $\varphi_1 = \angle(C_3,C_4,C_7,H_{10})$ and $\varphi_2 = \angle(C_2,C_1,C_{11},H_{14})$, corresponding to the internal rotations of the two methyl groups, were performed at the MP2/6-311++G(d,p) and B3LYP/6-311++G(d,p) levels of theory to study the coupling between the two tops by varying φ_1 and φ_2 in a grid of 10°. Due to symmetry, data points obtained in the range from φ_1 and φ_2 = 0° to 120° are sufficient. The corresponding energies were parameterized with a 2D Fourier expansion based on terms representing the correct symmetry. We used the Fourier coefficients summarized in Table S-3 to draw the PES as a contour plot illustrated in Fig. 2. Both PESs exhibit almost no potential coupling terms between φ_1 and φ_2. The experiment strongly supports this result since no potential coupling terms need to be included in the fits to

reproduce the observed rotational spectrum in the ground torsional state to measurement accuracy.

3. Spectral analysis

3.1. The *XIAM* and *PAM-C_{2v}-2tops* codes

To analyze the microwave spectra of DMF, we used two different codes which can deal with two-equivalent-top internal rotor problems. The first code is *XIAM* which has been described several times in the literature [5]. *XIAM* is a combined axis method which sets up the rotation-torsion Hamiltonian in the rho-axis system (RAM) for each top, then converts the RAM parameters into the principal axis system (PAM) parameters.

The second code, *PAM-C_{2v}-2tops*, has been recently developed to fit the high-resolution torsion-rotational spectra of molecules with two equivalent methyl rotors and a C_{2v} symmetry at equilibrium [6], which was successfully applied to acetone, CH_3COCH_3 [6,18]. It makes use of an explicit 2D potential function and allows simultaneous fitting of rotational transitions belonging to different torsional states of the molecule. *PAM-C_{2v}-2tops* is based on the G_{36} permutation-inversion (PI) group-theoretical considerations, and uses the principal axis method and a two-step diagonalization procedure. For blockwise diagonalization of a two-top torsion-rotational Hamiltonian, instead of the full G_{36} PI group, the G_9 PI group is used that splits the Hamiltonian matrix into four submatrices corresponding to the (00), (01), (11), and (12) symmetry species. These (00), (01), (11), and (12) blocks correspond to the ($A_1 \oplus A_2 \oplus A_3 \oplus A_4$), G, ($E_3 \oplus E_4$), and ($E_1 \oplus E_2$) symmetry species in G_{36}, respectively. A more detailed description of the program and the underlying group theory can be found in Ref. [6].

3.2. Microwave spectrum

The rotational spectrum of DMF was measured using two molecular jet FTMW spectrometers which cover the frequency range from 2 – 40 GHz. The spectrometer located in Aachen, Germany, operates from 2 – 26.5 GHz [19] and the other one in Paris, France, subsequently from 26.5 – 40 GHz [20]. DMF was purchased from Alfa Aesar GmbH & Co KG, Karlsruhe, Germany, and used without further purification. The stated purity is more than 98 %. The substance is a clear, volatile liquid. Its vapor pressure of approximately 50 hPa at 20°C is high and therefore simplified the measurement process. For all measurements, we used a gas mixture containing 1% DMF in helium at a total pressure of 60 to 110 kPa.

The spectrometers can operate in two different modes, the high resolution mode and the scan mode, where a series of overlapping spectra are automatically recorded in a step size of 0.25 MHz, and only the presence of lines is indicated in a broadband scan. In the high resolution mode, all lines appear as doublets due to the Doppler effect with the molecular transition frequency being the center frequency. The splitting depends on both, the frequency range and the velocity of the jet. The estimated measurement accuracy for rather strong unblended lines is better than 2 kHz [21]. For a number of lines, we observed additional splittings or excessive line broadening, probably because of spin-spin and/or spin rotation couplings of the protons in the molecule. Such lines were assigned with a measurement uncertainty of 8 kHz. In the fits, the weights are proportional to reciprocal of the squared measurement uncertainties.

As mentioned in Section 2.2., DMF belongs to the molecular symmetry group G_{36}, which is the same group as for 2,5-dimethylthiophene. Therefore, the selection rules for 2,5-dimethylthiophene can be applied directly for DMF, and we expect only *b*-type transitions in the spectrum [13]. This is in agreement with the calculated dipole moment components of 0.00 D, 0.31 D, and 0.00 D in *a*-, *b*-, and *c*-directions, respectively.

In the first step, the *b*-type rigid-rotor spectrum was predicted with the program *XIAM*, where we only considered the (00) torsional state. Based on this prediction, we measured several discontinuous broadband scans from 9.0 to 16.0 GHz. Afterwards, all lines were remeasured at higher resolution. Because the total dipole moment of 0.31 D is quite low, the measurements for DMF are more time consuming than usual since they require more decays to be averaged.

Because the prediction was sufficiently good, we could readily assign the *R*-branch $2_{12} \leftarrow 1_{01}$ and $3_{13} \leftarrow 2_{02}$ transitions as well as the *Q*-branch $3_{21} \leftarrow 3_{12}$, $4_{22} \leftarrow 4_{13}$ and $5_{23} \leftarrow 5_{14}$ transitions. These five transitions enabled us to determine all three rotational constants, and to predict and measure further rigid-rotor lines lying outside the broadband scans. The rigid-rotor fit including 49 rotational transitions (all of them belong to the (00) torsional species) is given as Fit (00) in Table 1.

In the next step, we carried out a prediction considering the internal rotations of both methyl groups, where each rotational transition is split into four torsional components. The angles between the internal rotor axes and the *a*-principal axis of inertia as well as the equivalent V_3 potentials were taken from *ab initio* calculations.

Based on the frequencies given in this prediction, we could assign the (01), (11), and (12) torsional species straightforwardly. The assignment was strongly supported by the intensities calculated with the spin statistical weights already given by group theory for the sulfur-analogue of DMF, 2,5-dimethylthiophene [13], i.e. (00) : (01) : (11) : (12) = 36 : 64 : 20 : 16 and 28 : 64 : 12 : 16 for ee $\leftrightarrow$ oo and eo $\leftrightarrow$ oe transitions, respectively. A typical spectrum with all four torsional components is illustrated in Fig. 3. In total, 193 torsion-rotational transitions of the ground torsional state up to $J = 11$ and $K_a = 5$ were measured and fitted with the program *XIAM*. The same set of transitions was also fitted using the *PAM-*C_{2v}*-2tops* code. These lines are almost evenly distributed between all four symmetry species,

except for some high J and K transitions where the (12) transitions are weak. We note that due to torsion-rotation mixing some nominal *c*-type transitions of the (01) and (12) torsional species, which would be forbidden in the rigid rotor approximation, are present, while no *a*-type forbidden ones are observable in this case. We found the same effect in our previous study on 2,5-dimethylthiophene [13]. In the case of ethyl methyl ketone, a molecule with C_s symmetry and two inequivalent methyl rotors, forbidden *c*-type transitions also occur for some (01), (10), and (12) torsional transitions due to the same reasons [22]. There are many further examples for one-top cases, where forbidden *c*-type transitions are present for C_s molecules; all of which are $|\sigma\rangle = |\pm 1\rangle$ species lines [23-25].

4. Results of the fits and discussion

The *XIAM* code reproduces 193 torsion-rotational transitions of DMF to a root-mean-square (rms) deviation of 2.2 kHz, which is almost the measurement accuracy. The rotational constant A, B, C, the centrifugal distortion constants Δ_J, Δ_{JK}, Δ_K, δ_J, δ_K, the V_3 potentials, and the angles between the internal rotation axes and the *a*-principal axis were determined with high accuracy, while the rotational constants of the two equivalent tops F_0 were kept fixed to the *ab initio* values. In agreement with the results of quantum chemical calculations given in Section 2.3., potential coupling terms are not necessary to achieve this fit quality. The fit is given as Fit *XIAM* in Table 1.

The *PAM-C_{2v}-2tops* code provides a fit of similar quality (rms = 2.2 kHz, weighted rms = 0.9) by floating 12 parameters, which are the three rotational and five centrifugal distortion constants, the V_3 barrier height, the two parameters associated with the ρ_z and ρ_x components of the rho vector, and a parameter of the J dependence of the barrier height. The Cartesian components of the rho vector are given by $\rho_{gn} = \lambda_{gn} I_{\alpha n}/I_g$ with the principal axes of inertia $g \in \{x, y, z\}$ and the top n = A, B, where λ_{gn} is the direction cosine between the g axis and the internal rotor axis, $I_{\alpha n}$ the moment of inertia of top n, and I_g the principal moment of

inertia of the molecule. The internal rotation constants for the two equivalent tops were also kept fixed to values derived from *ab initio*. This parameter could not be determined because the present data set contains only information on the torsional ground state with relatively low J and K values, and because the torsional barrier is rather high ($s = 4V_3/9F \approx 35.5$). Some of the parameters fitted by *PAM-C_{2v}-2tops* (recalculated if necessary) are compared with the *ab initio* and *XIAM* values in the fifth column of Table 1 (Fit *PAM-C_{2v}*); other parameters are given in the footnote of Table 1 as well as in Table S-4 in the Supplementary Material. The list of frequencies fitted with the *PAM-C_{2v}-2tops* and *XIAM* codes, along with their residuals, is available in Table S-5.

Both *PAM-C_{2v}-2tops* and *XIAM* are suitable to analyze the spectrum of DMF to measurement accuracy. The rotational constants obtained with both programs agree well; however, they do not agree within the standard errors because different sets of parameters were fitted. The experimentally deduced rotational constants are compared with those from quantum chemical calculations performed at different levels of theory (see Table S-2). At almost all levels, the differences between the experimental and calculated B and C rotational constants are smaller than for the A rotational constant. We emphasize that quantum chemical data refer to the equilibrium structure, whereas the experimental data yield rotational constants for the ground vibrational state and no corrections have been made. Only at the MP2/6-311++G(d,p) level of theory, we carried out anharmonic frequency calculations to provide the ground state r_0 structure and to calculate the centrifugal distortion constants. The A_0, B_0, and C_0 rotational constants are given in Table 1. In contrast to our expectation, these values are not in better agreement with the experimental values than the A_e, B_e, and C_e values obtained at some levels of theory listed in Table S-2.

The centrifugal distortion constants deduced by the *PAM-C_{2v}-2tops* and *XIAM* codes are similar, except for the δ_K parameter (see Table 1). These constants are predicted well with the MP2/6-311++G(d,p) level, whereby the calculated values are closer to the *XIAM* values

than those of *PAM-C_{2v}-2tops*. Since the ring frame of DMF is quite rigid, all centrifugal distortion constants are small.

Both *PAM-C_{2v}-2tops* and *XIAM* yield very similar V_3 potentials of approximately 439 cm^{-1}, which are much higher than the value of 247.95610(30) cm^{-1} of the sulfur analog 2,5-dimethylthiophene [13]. The same trend is observed for the monomethyl derivatives of furan and thiophene, e.g. 2-methylfuran (416.2 cm^{-1}) [26] versus 2-methylthiophene (194.1 cm^{-1}) [27] and 3-methylfuran (380.5 cm^{-1}) [28] versus 3-methylthiophene (258.8 cm^{-1}) [29].

Furthermore, we also compare the angles between the internal rotor axes and the *a*-principal axis. Similar to the difference between H_2O and H_2S, the $\angle$(i,*a*) angle of 27.2840(85)° in DMF is significantly larger than the value of 14.5931(78)° found for 2,5-dimethylthiophene [13], as visualized in Fig. 4, in which the optimized conformers calculated at the MP2/6-311++G(d,p) level for both molecules are superposed.

The V_3 potentials calculated for DMF using the MP2, M06-2X, and B3LYP methods are between 362.2 − 421.6 cm^{-1}, in the same order of magnitude as the experimental values. Using the HF method, this value is always overestimated by about 100 cm^{-1}, lying in the range between 500 − 600 cm^{-1} (see Table S-2).

The inertial defect $\Delta_c = (I_c - I_a - I_b)$ = –6.280 u$Å^2$ confirms that the heavy atom skeleton is planar with two pairs of hydrogen atoms out of plane. This value is essentially the same as that found in 2,5-dimethylthiophene (Δ_c = –6.275 u$Å^2$) [13] and other rings containing two methyl groups with comparable barrier heights, e.g. 3,5-dimethylbenzaldehyde (Δ_c = –6.245 u$Å^2$) [30] and the two conformers of 2-acetyl-5-methylfuran (Δ_c = –6.469 and –6.508 u$Å^2$ for the *trans* and *cis* conformers, respectively) [15]. In all these cases the barriers to internal rotation are sufficiently high, so that the observed inertial defects are almost those of rigid molecules.

5. Conclusion

The only existing conformer of 2,5-dimethylfuran under molecular jet conditions was studied using a combination of FTMW spectroscopy and quantum chemistry. The high resolution of our experimental technique allowed us to resolve completely torsional splittings arising from the internal rotations of two equivalent methyl groups with a barrier height of 439.1626(71) cm^{-1}. The assigned spectrum was fitted using the *XIAM* and *PAM-C_{2v}-2tops* programs, which reproduced the data set to measurement accuracy (2 kHz). Accurate molecular parameters were determined from the analysis of the observed spectrum, and their values agree well with the results of quantum chemical calculations. The angles between internal rotor axes and the *a*-principal axis of DMF differ by 12.7° from those of the sulfur analog 2,5-dimethylthiophene.

Acknowledgements

V.V. thanks the Fonds der Chemischen Industrie (FCI) for a Ph.D. fellowship. Simulations were performed with computing resources granted by JARA-HPC from the RWTH Aachen University under the project jara0124.

References

[1] A. Y. Román-Leshkov, C. J. Barrett, Z. Y. Liu, J. A. Dumesic, Nature 447 (2009) 982.

[2] M. Chidambaram, A. T. Bel, Green Chem. 12 (2010) 1253.

[3] T. Thananatthanachon, T. B. Rauchfuss, Angew. Chem. Int. Ed. 49 (2010) 6616.

[4] J. B. Binder, R. T. Raines, J. Am. Chem. Soc. 131 (2009) 1979.

[5] H. Hartwig, H. Dreizler, Z. Naturforsch. 51a (1996) 923.

[6] V. V. Ilyushin, J. T. Hougen, J. Mol. Spectrosc. 289 (2013) 41.

[7] M. J. Frisch, G. W. Trucks, H. B. Schlegel, G. E. Scuseria, M. A. Robb, J. R. Cheeseman, G. Scalmani, V. Barone, B. Mennucci, G. A. Petersson, H. Nakatsuji, M. Caricato, X. Li, H. P. Hratchian, A. F. Izmaylov, J. Bloino, G. Zheng, J. L. Sonnenberg, M. Hada, M. Ehara, K. Toyota, R. Fukuda, J. Hasegawa, M. Ishida, T. Nakajima, Y. Honda, O. Kitao, H. Nakai, T. Vreven, J. A. Montgomery, Jr., J. E. Peralta, F. Ogliaro, M. Bearpark, J. J. Heyd, E. Brothers, K. N. Kudin, V. N. Staroverov, R. Kobayashi, J. Normand, K. Raghavachari, A. Rendell, J. C. Burant, S. S. Iyengar, J. Tomasi, M. Cossi, N. Rega, J. M. Millam, M. Klene, J. E. Knox, J. B. Cross, V. Bakken, C. Adamo, J. Jaramillo, R. Gomperts, R. E. Stratmann, O. Yazyev, A. J. Austin, R. Cammi, C. Pomelli, J. W. Ochterski, R. L. Martin, K. Morokuma, V. G. Zakrzewski, G. A. Voth, P. Salvador, J. J. Dannenberg, S. Dapprich, A. D. Daniels, O. Farkas, J. B. Foresman, J. V. Ortiz, J. Cioslowski and D. J. Fox, Gaussian 09, Revision A.02, Gaussian, Inc., Wallingford CT, 2009.

[8] R. Kannengießer, W. Stahl, H. V. L. Nguyen, W. C. Bailey, J. Mol. Spectrosc. 317 (2015) 50.

[9] R. Kannengießer, W. Stahl, H. V. L. Nguyen, J. Phys. Chem. A 120 (2016) 5979.

[10] V. Van, W. Stahl, H. V. L. Nguyen, J. Mol. Struct. 1123 (2016) 24.

[11] R. Ditchfield, W. J. Hehre, J. A. Pople, J. Chem. Phys. 54 (1971) 724.

[12] T. H. Dunning Jr., J. Chem. Phys. 90 (1989) 1007.

[13] V. Van, W. Stahl, H. V. L. Nguyen, Phys. Chem. Chem. Phys. 17 (2015) 32111.

[14] A. Jabri, V. Van, H. V. L. Nguyen, W. Stahl, I. Kleiner, ChemPhysChem 17 (2016) 2660.

[15] V. Van, W. Stahl, H. V. L. Nguyen, ChemPhysChem 17 (2016) 3223.

[16] R. Kannengießer, S. Klahm, H. V. L. Nguyen, A. Lüchow, W. Stahl, J. Chem. Phys. 141 (2014) 204308.

[17] H. B. Schlegel, J. Comput. Chem. 3 (1982) 214.

[18] I. A. Armieieva, V. V. Ilyushin, E. A. Alekseev, O. A. Dorovskaya, L. Margulès, R. A. Motiyenko, Radio Phys. Radio Astron. 21 (2016) 37.

[19] J.-U. Grabow, W. Stahl, H. Dreizler, Rev. Sci. Instrum. 67 (1996) 4072.

[20] I. Merke, W. Stahl, H. Dreizler, Z. Naturforsch. 49a (1994) 490.

[21] J.-U. Grabow, W. Stahl, Z. Naturforsch. 45a (1990) 1043.

[22] H. V. L. Nguyen, V. Van, W. Stahl, I. Kleiner, J. Chem. Phys. 140 (2014) 214303.

[23] H. V. L. Nguyen, A. Jabri, V. Van, W. Stahl, J. Phys. Chem. A 118 (2014) 12130.

[24] L. Ferres, W. Stahl, I. Kleiner, H. V. L. Nguyen, J. Mol. Spectrosc. (2017). DOI: 10.1016/j.jms.2017.09.008

[25] R. Kannengießer, W. Stahl, H.V.L. Nguyen, I. Kleiner, J. Phys. Chem. A 120 (2016) 3992.

[26] W. G. Norris, L. C. Krisher, J. Chem. Phys. 51 (1969) 403.

[27] N. M. Pozdeev, L. N. Gunderova, A. A. Shapkin, Opt. Spektrosk. 28 (1970) 254.

[28] T. Ogata, K. Kozima, Bull. Chem. Soc. Jpn. 44 (1971) 2344.

[29] T. Ogata, K. Kozima, J. Mol. Spectrosc. 42 (1972) 38.

[30] M. Tudorie, I. Kleiner, M. Jahn, J.-U. Grabow, M. Goubet, O. Pirali, J. Phys. Chem. A 117 (2013) 13636.

Table 1. Spectroscopic constants of DMF referred to the PAM system.

Par.	Unit	Fit (00)[a]	Fit XIAM[a]	Fit PAM-C_{2v}[b]	MP2[c]
A	GHz	6.16146634(21)	6.16068435(13)	6.16102(11)	6.053
B	GHz	2.13078096(12)	2.130807556(70)	2.131127(55)	2.120
C	GHz	1.615040197(77)	1.614988865(51)	1.615296(40)	1.602
Δ_J	kHz	0.1259(11)	0.12463(56)	0.12411(46)	0.1210
Δ_{JK}	kHz	−0.2918(49)	−0.3300(29)	–0.3730(25)	−0.3216
Δ_K	kHz	3.6972(58)	3.4048(39)	3.4477(33)	3.3497
δ_J	kHz	0.03916(66)	0.03848(32)	0.03834(25)	0.03819
δ_K	kHz	0.154(13)	0.1494(78)	0.27142(66)	0.13773
V_3	cm^{-1}		439.1461(83)	439.1626(71)	404.1
F_0	GHz		159.382[d]		159.382
F	GHz		165.02[e]	165.02[e]	164.97
$\angle(i_A,a)$[f]	°		27.2840(85)		27.32
$\angle(i,b)$	°		62.7160(85)		62.68
$\angle(i,c)$	°		90.0[g]		90.00
rms[h]	kHz	1.5	2.2	2.2	
N[i]		49	193	193	

[a] All parameters refer to the principal axis system. Watson's A reduction Hamiltonian in I^r representation was used. [b] Recalculated from the *PAM-C2v-2tops* parameters. The fitted effective A and B rotational constants are $A_{eff} = A + 2F\rho_z^2 = 6.550582(86)$ GHz, $B_{eff} = B + 2F\rho_x^2 = 2.143537(51)$ GHz. Three additional parameters are $4F\rho_z = (1/2)(p_A - p_B)J_z = 22.6776(19)$ GHz, $4F\rho_x = (1/2)(p_A + p_B)J_x = 4.0476(37)$ GHz, and $V_{3J} = (1/2)(1-\cos 3\alpha_A + 1 - \cos 3\alpha_B)J^2 = -1.90(24)$ MHz, where the expression between the parameter and its value gives the operator which multiplies this parameter in the fit. [c] Ground state rotational constants and centrifugal distortion constants obtained by anharmonic frequency calculation at the MP2/6-311++G(d,p) level of theory. [d] Fixed to the *ab initio* value. [e] Derived parameter in *XIAM*, fixed in *PAM-C2v-2tops*. [f] $\angle(i_B,a) = 180° - \angle(i_A,a)$. [g] Fixed due to symmetry. [h] Root-mean-square deviation of the fit. [i] Number of lines.

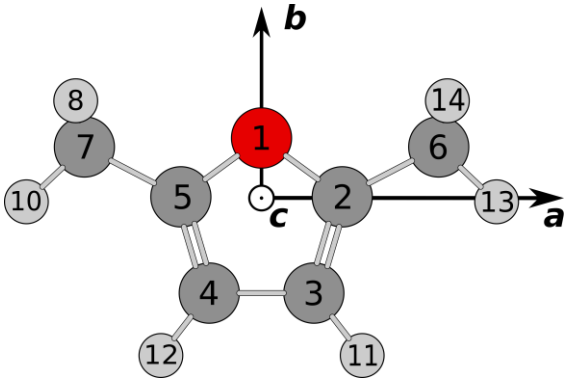

Fig. 1. The equilibrium geometry of DMF optimized at the MP2/6-311++G(d,p) level of theory given in its principal axes of inertia. The direction of the *c*-axis out of the paper plane is indicated by an encircled dot. The protons H_9 and H_{15} are located behind H_8 and H_{14}, respectively.

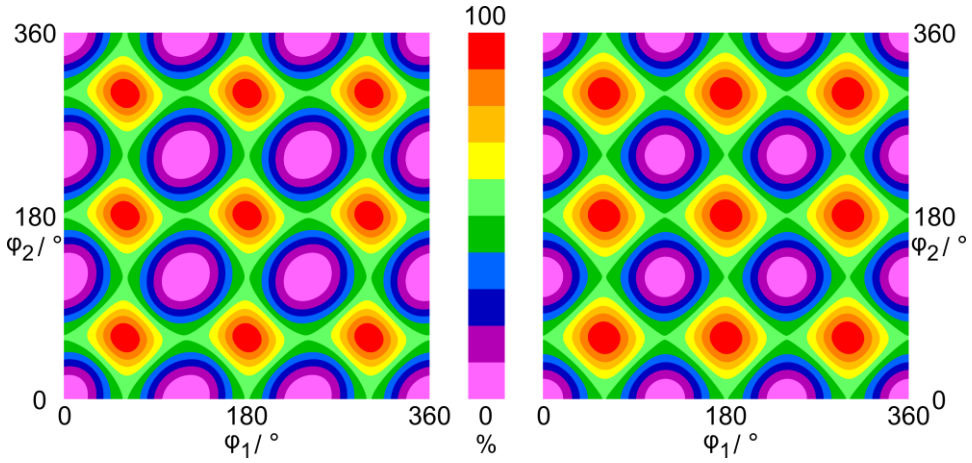

Fig. 2. The potential energy surfaces of DMF depending on the dihedral angles $\varphi_1 = \angle(C_3,C_4,C_7,H_{10})$ and $\varphi_2 = \angle(C_2,C_1,C_{11},H_{14})$ calculated at the MP2/6–311++G(d,p) (left) and B3LYP/6–311++G(d,p) levels of theory (right). The angles φ_1 and φ_2 were varied in a grid of 10°, while all other parameters were optimized. The color code indicates the energies (in per cent) relative to those of the energetically lowest conformations with E_{min} = –307.8437029 (MP2) and –308.7532858 Hartree (B3LYP) (0%). The energy maxima (100%) are E_{max} = –307.8400386 and –308.7496142 E_h, respectively.

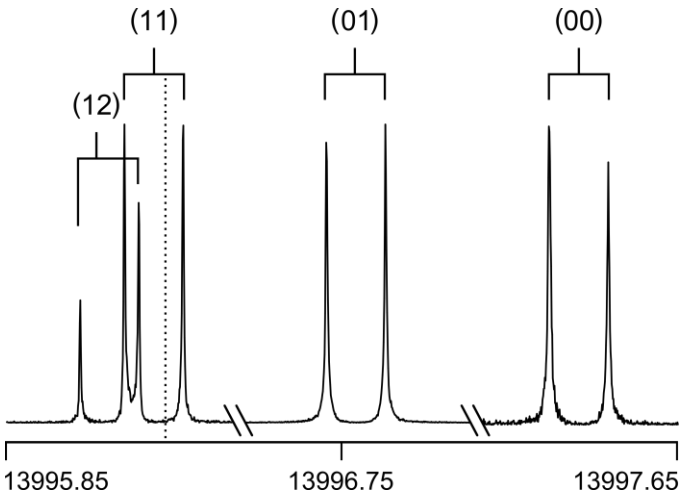

Fig. 3. High resolution spectra (in MHz) showing four torsional species (00), (01), (11), and (12) of the $3_{13} \leftarrow 2_{02}$ transition of DMF, where the intensities are normalized for each frequency section. The splittings indicated by brackets are due to the Doppler effect. The polarization frequency of the lowest frequency section is given as a dashed line. For these spectra (from the left to the right hand side), 153, 202, and 203 decays, respectively, are co-added. The spin statistical weight of the (00) species is only half of that of the (01) species (see text). Therefore, at the same number of co-added decays, there is more noise visible for the (00) transition.

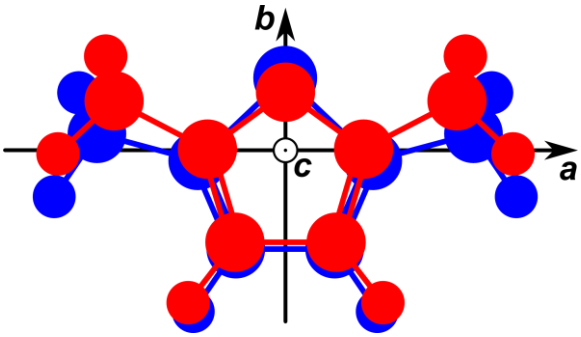

Fig. 4. The observed conformer of 2,5-dimethylthiophene (blue) and DMF (red) the principal axes of inertia optimized at the MP2/6-311++G(d,p) level, showing that (i) the sulfur atom in 2,5-dimethylthiophene is located higher on the *b*-axis than the oxygen atom in DMF and (ii) the angles $\angle$(i,*a*) of the molecules differ by 12.7°.